



Results of the in-beam tests performed with the quadrant 0 of station 1 for the ALICE dimuon arm

M-P. Comets, P. Courtat, C. Diarra, B. Espagnon, R. Guernane, D. Guez, I. Hrivnacova, R. Kunne, Y. Le Bornec, M. Mac Cormick, et al.

► To cite this version:

M-P. Comets, P. Courtat, C. Diarra, B. Espagnon, R. Guernane, et al.. Results of the in-beam tests performed with the quadrant 0 of station 1 for the ALICE dimuon arm. 2003, pp.17. in2p3-00014023

HAL Id: in2p3-00014023

<https://hal.in2p3.fr/in2p3-00014023>

Submitted on 30 Sep 2003

HAL is a multi-disciplinary open access archive for the deposit and dissemination of scientific research documents, whether they are published or not. The documents may come from teaching and research institutions in France or abroad, or from public or private research centers.

L'archive ouverte pluridisciplinaire **HAL**, est destinée au dépôt et à la diffusion de documents scientifiques de niveau recherche, publiés ou non, émanant des établissements d'enseignement et de recherche français ou étrangers, des laboratoires publics ou privés.

RESULTS OF THE IN-BEAM TESTS PERFORMED WITH THE QUADRANT 0 OF STATION 1 FOR THE ALICE DIMUON ARM

M.P. Comets, P. Courtat, C. Diarra, B. Espagnon, R. Guernane, D. Guez,
I. Hrivnacova, R. Kunne, Y. Le Bornec, M. Mac Cormick,
J.M. Martin, S. Rousseau and N. Willis

Institut de Physique Nucléaire d'Orsay (IPNO)
IN2P3/CNRS and Université Paris-Sud
BP n^o1 F-91406 Orsay - FRANCE

P. Bhattacharya, S.Chattopadhyay, N. Majumdar and P. Roy

Saha Institute of Nuclear Physics
1/AF, Bidhan Nagar, Kolkata – 700064 INDIA

V. Nikulin
PNPI RAS, Gatchina,
Leningrad district, 188350- RUSSIA

Abstract: In-beam tests have been carried out on the first final quadrant of station 1 on the PS beam line in July 2002. Studies of gain, homogeneity of the response and resolution have been performed and the results are reported here.

The first quadrant of the Station 1 has been constructed at IPN Orsay by RDD (Research and Development in Detectors) and SEP (Service d'électronique Physique) departments. This quadrant was supposed to be a definitive chamber and, thus, to have all the final geometrical parameters:

- Rmin = 182 mm
- Rmax = 883 mm
- anode-cathode gap = 2.1 mm
- anode pitch = 2.1 mm
- wire diameter = 20 μ m
- pad sizes:
 - in the bending plane
 - Rmin to R = 552 mm: 4.2 x 6.3 mm² (respectively along Y and X directions)
 - R = 552 mm to R = 713 mm: 4.2 x 12.6 mm²
 - R = 713 mm to R = 883 mm: 4.2 x 25.2 mm²
 - in the non-bending plane

- Rmin to R= 552 mm: $4.2 \times 6.3 \text{ mm}^2$ (respectively along Y and X directions)
- R= 552 mm to R = 713 mm : $8.4 \times 6.3 \text{ mm}^2$
- R= 713 mm to R = 883 mm : $16.8 \times 6.3 \text{ mm}^2$

In the most central zone, the pads have the same sizes in both cathode planes but are staggered by half a width and half a length. The signals are collected on the cathodes by groups of 64 pads and are transmitted to the FEE by means of kaptons with 80 wires (64 signals, 16 groundings).

A standard 80 % Ar- 20 % CO₂ gas mixture was used.

During this in-beam test, the quadrant was just equipped with a mother board (on which the FEE is plugged) in the non-bending plane which contains the numerical buses for the read-out and all the lines for the LV supplies and for the different signals (trigger, calibration...). A view of the quadrant can be seen in figure 1.

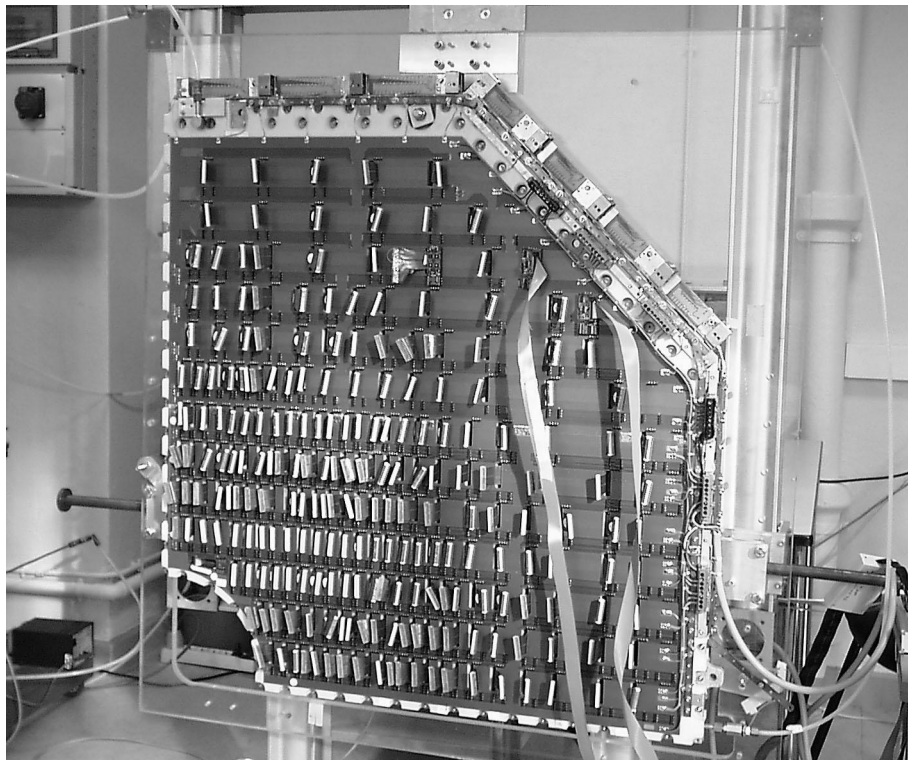


Figure 1: View of the quadrant 0

Some striking features of this quadrant will be presented in the following sections.

1- Leaks: It has been seen huge leaks after the closure of the chamber ($\sim 30 \text{ l/h}$). These leaks have been found to come through the vias in the cathode PCBs which were supposed to be filled by a varnish in the company in charge of the PCB production. This work has been badly done and the tightness has not been checked at IPN.

After some trials to repair the quadrant, the leakage rate has been decreased down to the level of ~ 6 l/h which is still far from being satisfactory. This default is well identified and will be corrected on the next quadrants.

2- FEE performances: During these tests, the quadrant was equipped with 26 MANUs modules (MANas NUMerical) which were moved with respect of the beam location. Each MANUs was composed of 4 GASSIPLEX $0.7\ \mu\text{m}$, 2 ADC 12 bits and a MARC2 chip. One of the challenges of the read-out system was the ability to read 26 MANUs (1664 channels) plugged on the same numerical bus (the most heavy loaded one) due to the adaptation of the signals. As it can be seen in figure 2, the read-out has perfectly worked.

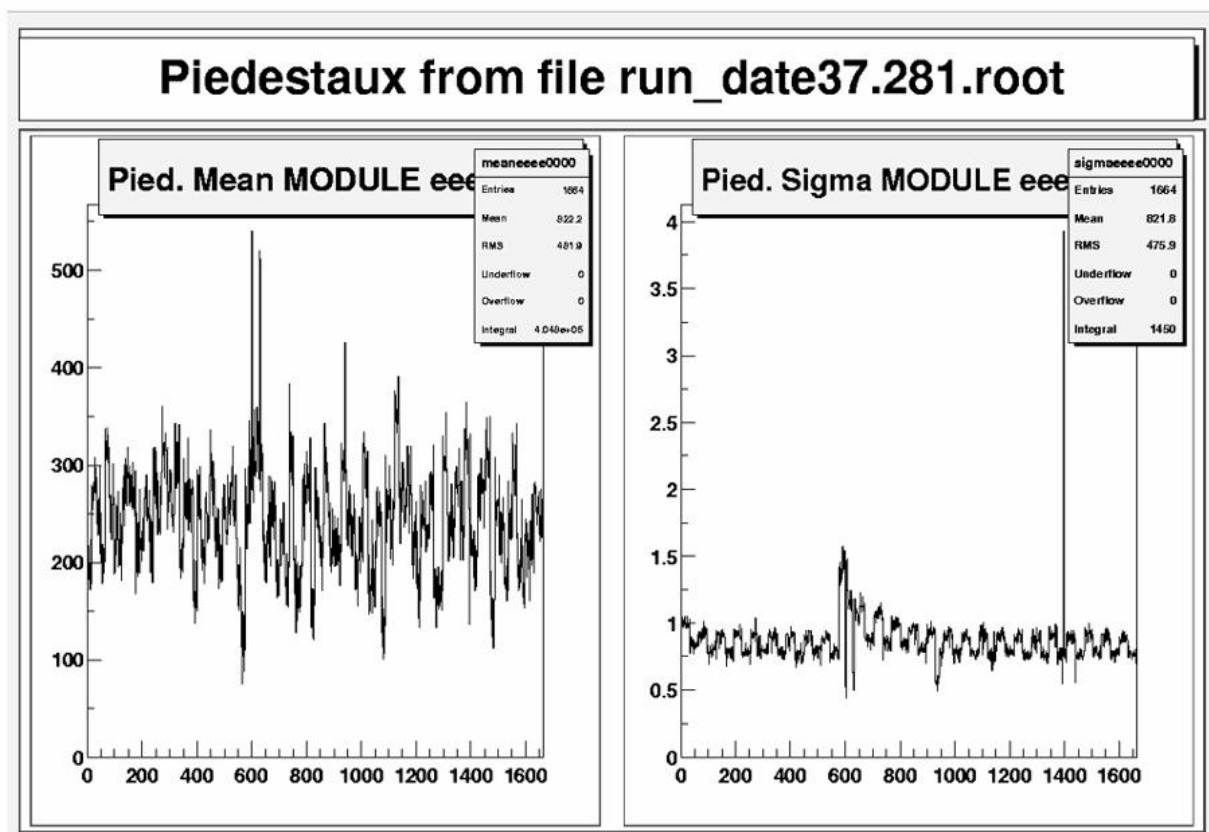


Figure 2: On the left part of the figure, histogram of the pedestals of the 1664 channels read on two numerical buses. On the right part, values of the noises measured for these same 1664 channels.

Some comments have to be done on the spectrum of the noises:

- the increase of the noise for the 64 channels around the channel 600 is due to a modification of the ADC reference which has been decreased down to 2.5 V instead of 3 V for all the others MANUs. The consequence is to artificially increase the noise by a factor $3/2.5=1.2$ in ADC channel number
- the decreasing slope starting around channel 600 is due to the capacitance variation due to the pad sizes variation
- the structure with a 32 channel periodicity is due to the layout of the MANUs. The reference voltages for the two ADC are driven by two lines with different lengths which induce different noises. This slight default has been corrected for the final version

The histogram of the pedestals and of the noise can be seen in figures 3 and 4.

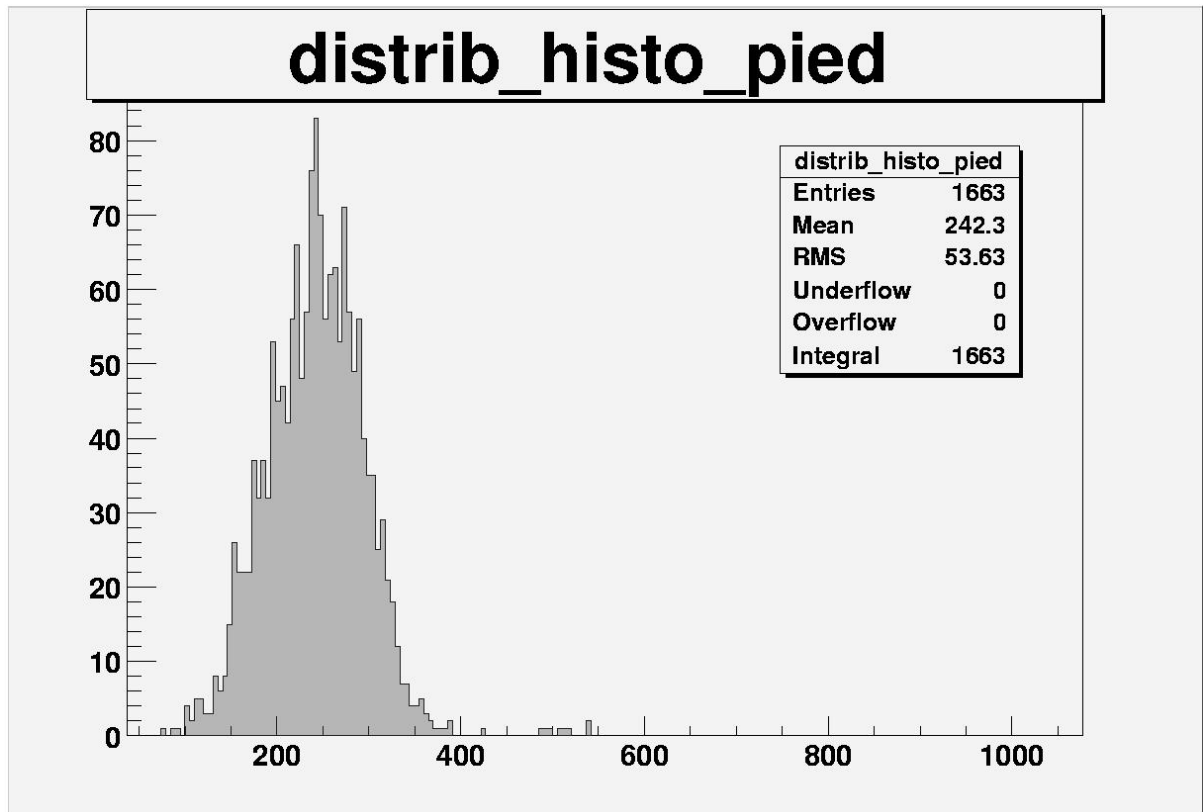


Figure 3: histogram of the GASSIPLEX pedestals digitised on 12 bits

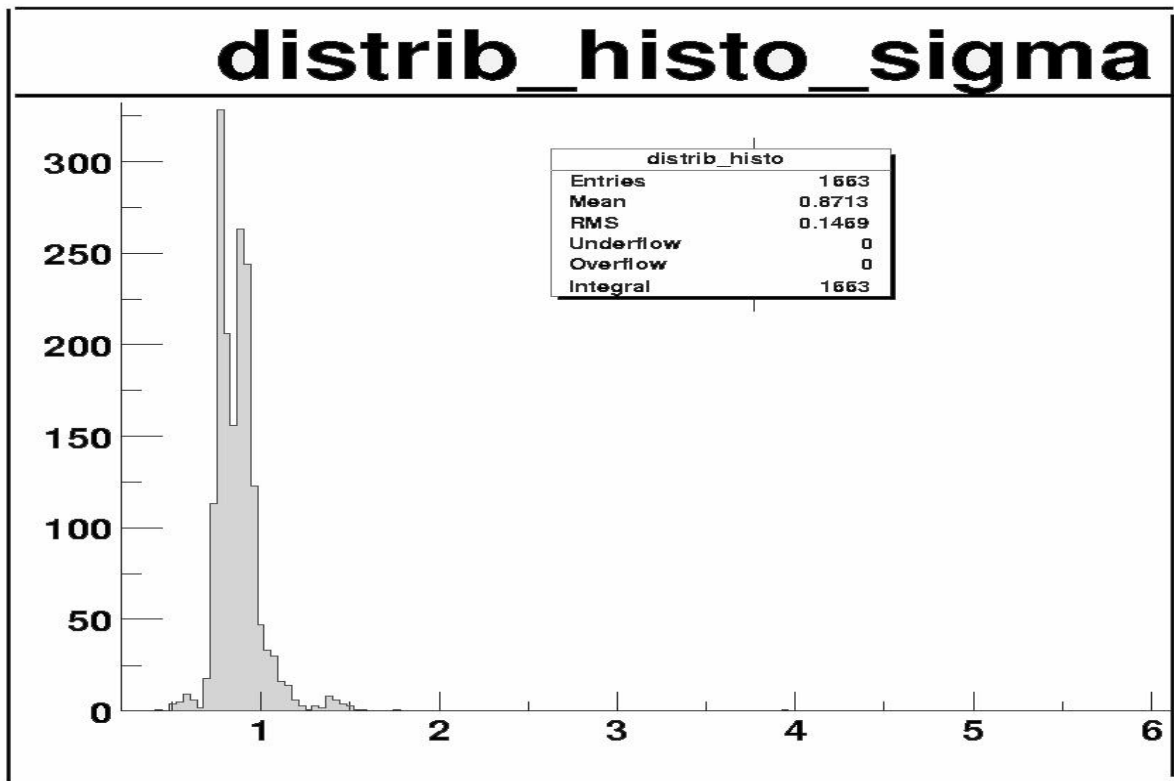


Figure 4: histogram of the electronics noise measured on 1664 channels digitised on 12 bits

Considering the GASSIPLEX gain of 3.5 mV/fC, the mean value of the noise (0.87 ADC channels) corresponds to 1125 electrons.

During the tests, a slow coherent variation of all the pedestal values has been observed as it can be seen in figure 5 where is plotted the variation at a given time. The variation versus time is given in figure 6.

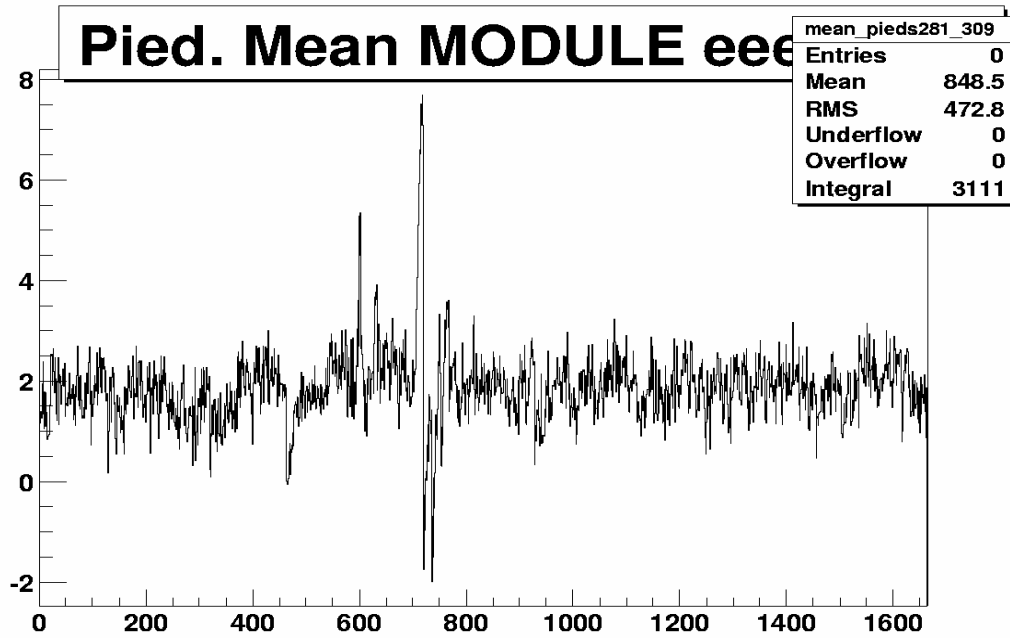


Figure 5: Value of the pedestal variation versus the channel number at a given time

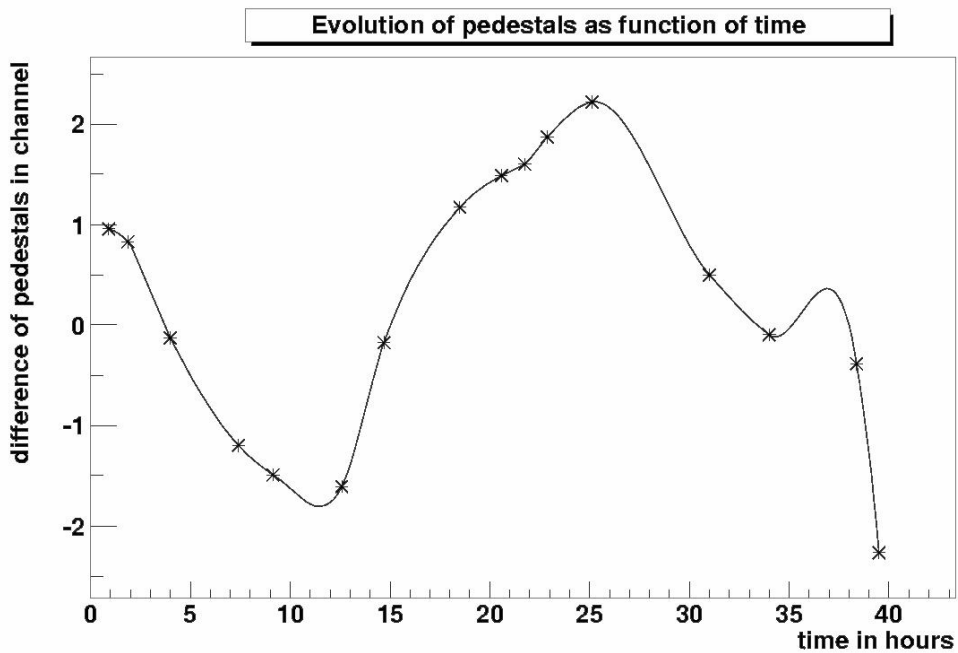


Figure 6: Mean pedestal value variation versus time

As we plugged and unplugged the MANUs for studying different zones, the experimental conditions were not stable enough to be able to draw definitive conclusions but, nevertheless, it seems that it exists a periodicity of 24 hours which could be due to a day/night effect (temperature, humidity...?).

More precise studies have been started to try to find the components responsible for such a variation. As an example, the pedestal shifts have been gathered for the 1664 channels modulo 64 channels (corresponding to one MANU structure). One can remark (figure 7) a periodical structure every 16 channels around a mean value of 1.8 channel. This suggests an individual GASSIPLEX effect.

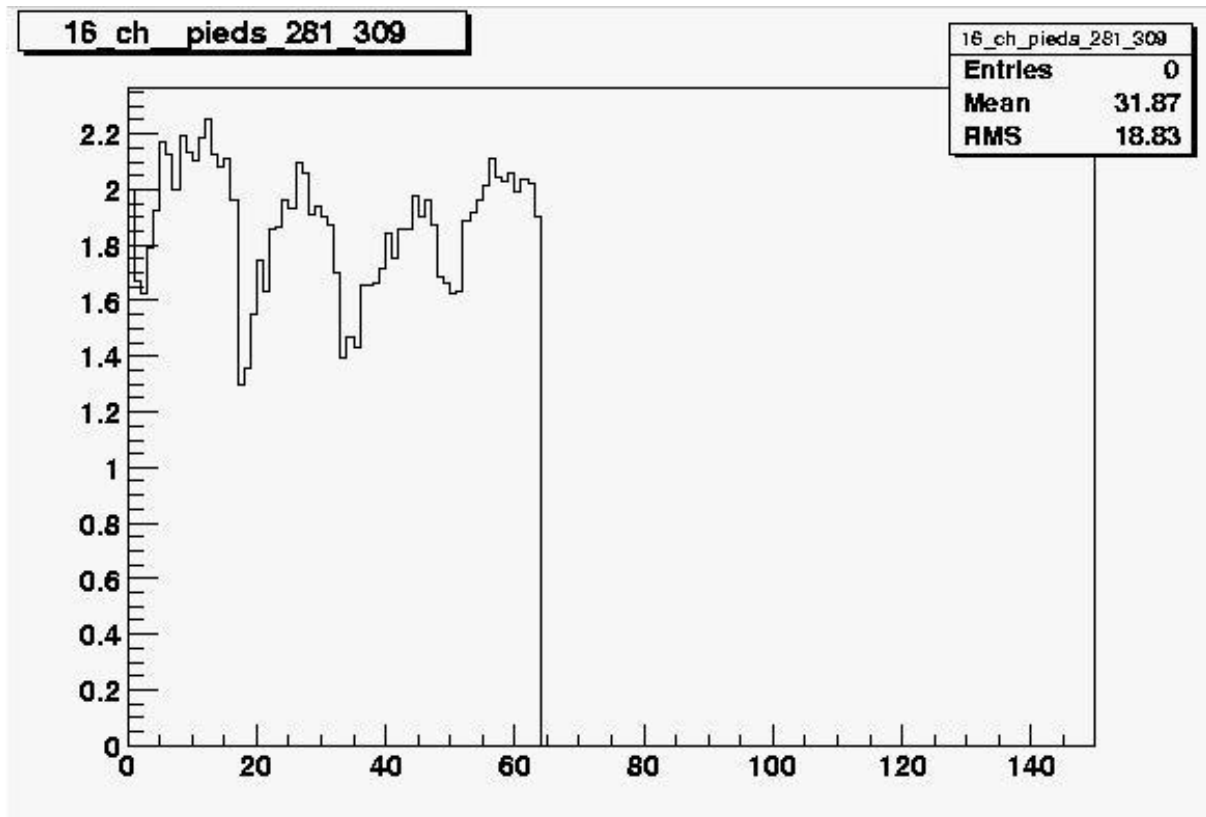


Figure 7: Pedestal shifts of 1664 channels drawn modulo 64

3- HV behaviour:

- the leakage current is very low, typically a few nA up to a high voltage value of about 1725 V
- it has been remarked that the leakage current increases with the atmosphere humidity. It seems that it is due to surface currents which can be easily decreased by means of a hair drier on the external PCBs. A slight modification of the HV circuit will be done to prevent from this default.

4- gain measurements: The chamber gain has been measured for different HV values, in different points which locations are shown in figure 8.

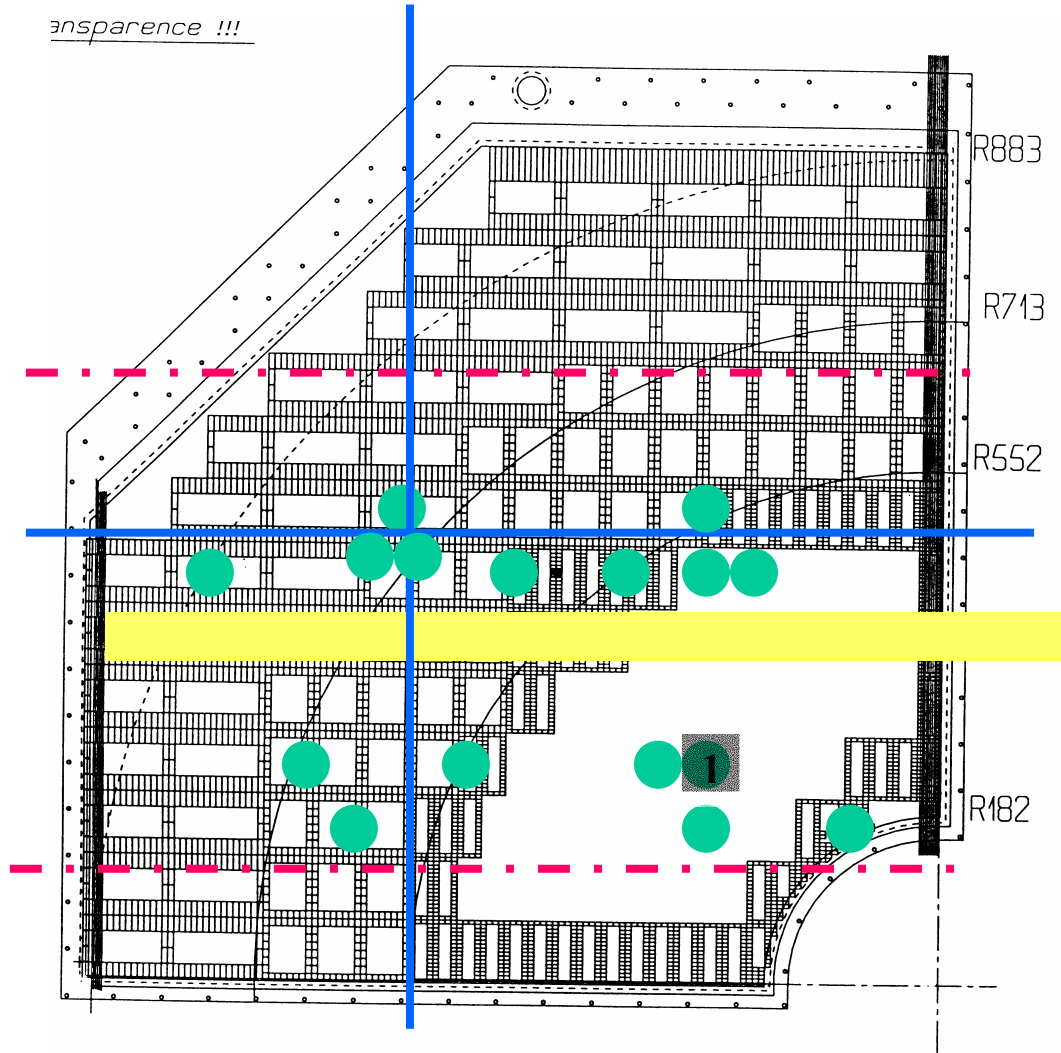


Figure 8: schematic view of the quadrant where the three concentric zones can be seen. The green spots correspond to the location of the measurements, the red lines delimitate the possible explored region and the blue line represents the cathode PCBs junction. As an example, the yellow row corresponds to one of the area equipped with a chained electronics

To evaluate the absolute gain, we have used the following inputs:

- 130 primary electrons/cm for 7 GeV/c pions
- GASSIPLEX gain: 3.5 mV/fC
- ADC: 3V for 4096 channels
- deficit due to the electronic integration time estimated to be 0.642.
- charge on the wire equal at twice the charge measured on one cathode
- the maximum of the Landau fit has been taken into account to estimate the number of electrons

A typical response of the chamber for HV=1700 V, obtained on point 1 of figure 8 is shown in figure 9.

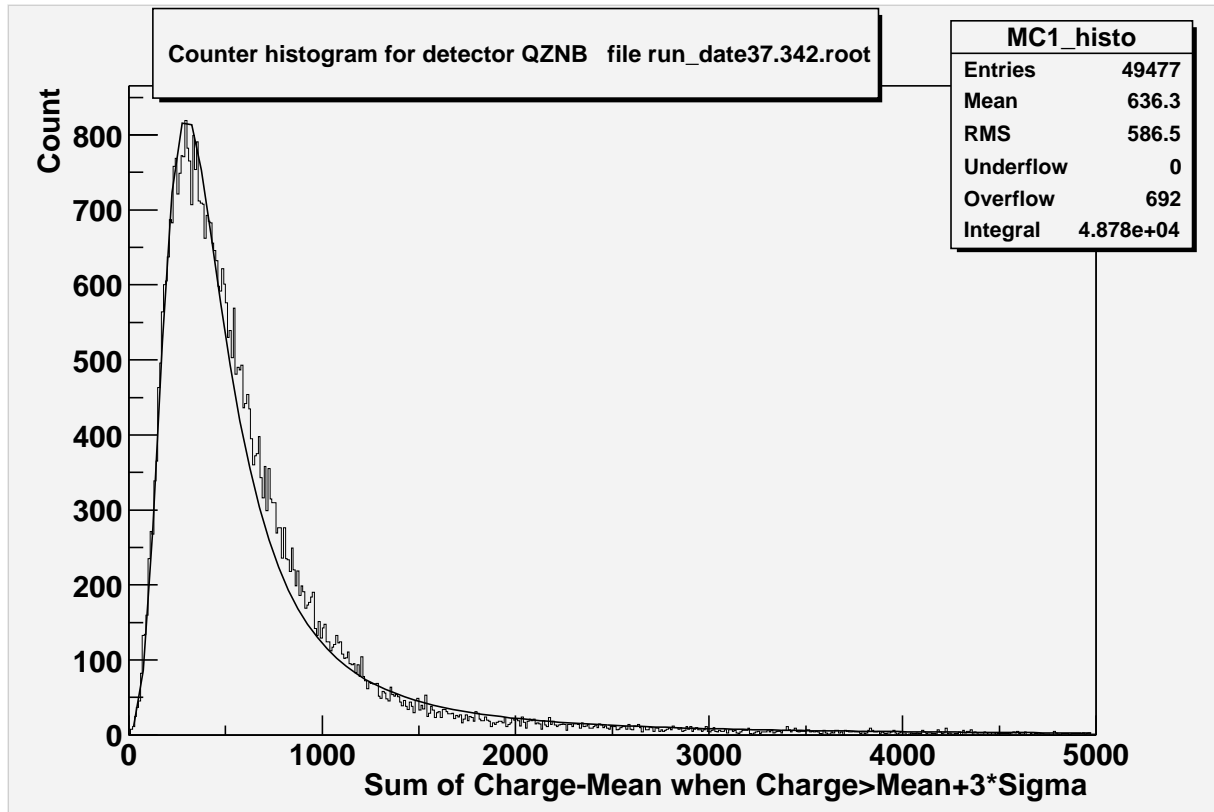


Figure 9: Total charge measured on the non-bending plane for HV = 1700 V

Results are presented for different HV values in table 1.

High Voltage (V)	1600	1650	1700
Gain	$7.6 \cdot 10^3$	$1.37 \cdot 10^4$	$2.44 \cdot 10^4$

Table 1: Gain values for different High Voltage settings

The experimental gains are plotted in figure 10, for the mock-up [1] (full blue circles) and for the quadrant (red squares). The two differences between these two detectors are the gap and the anode pitch of the mock-up (respectively 2 mm and 2.5 mm). To obtain the same gain on both detectors, a high voltage higher by 220 V has to be applied on the quadrant. Theoretical calculations carried out with GARFIELD code [2] show that only a 110 V shift is predicted to obtain the same gain. It seems that the gain of the quadrant is lower than the predicted value extrapolated from the mock-up one by a factor around 4.

These calculations of the absolute gains depend on the number of primary electrons which can vary of a factor about 1.5 following the different hypothesis.

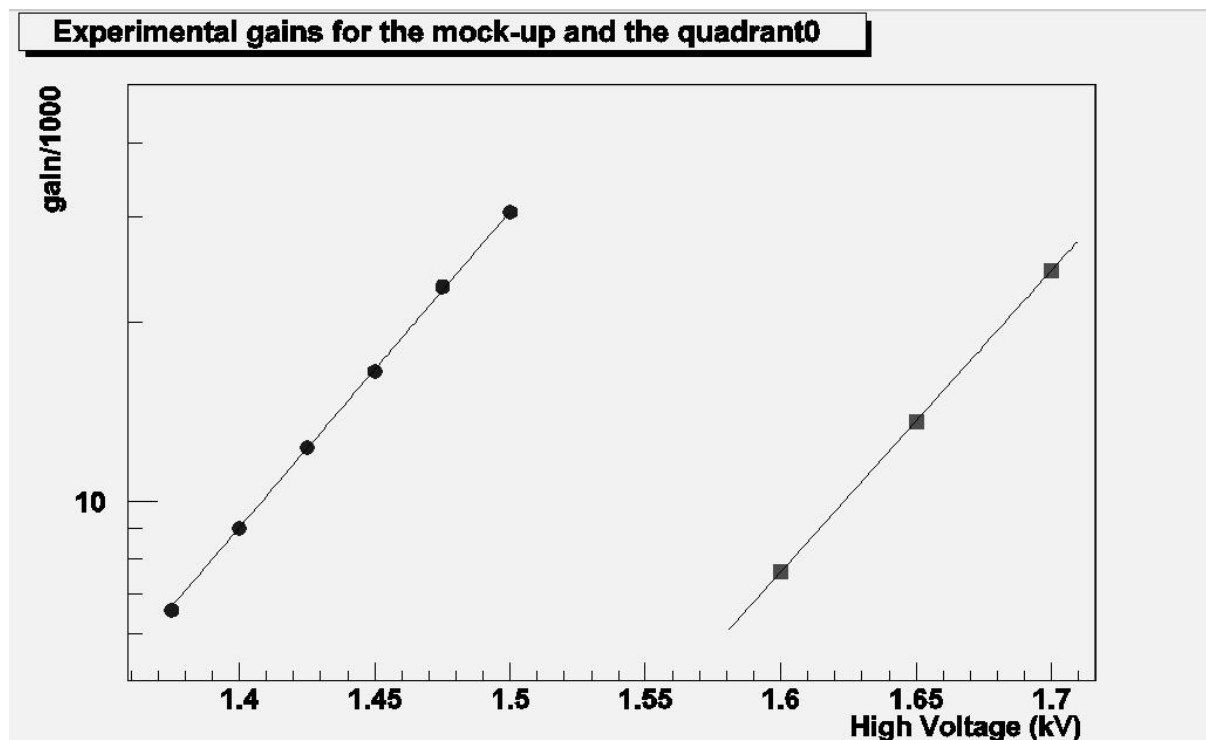


Figure 10: Experimental gains for the mock-up (blue circles) and the quadrant (red squares) versus the high voltage

5- Gain homogeneity: The gain has been measured for different points corresponding to different pad geometries. The results are shown in figure 11 for different high voltage values.

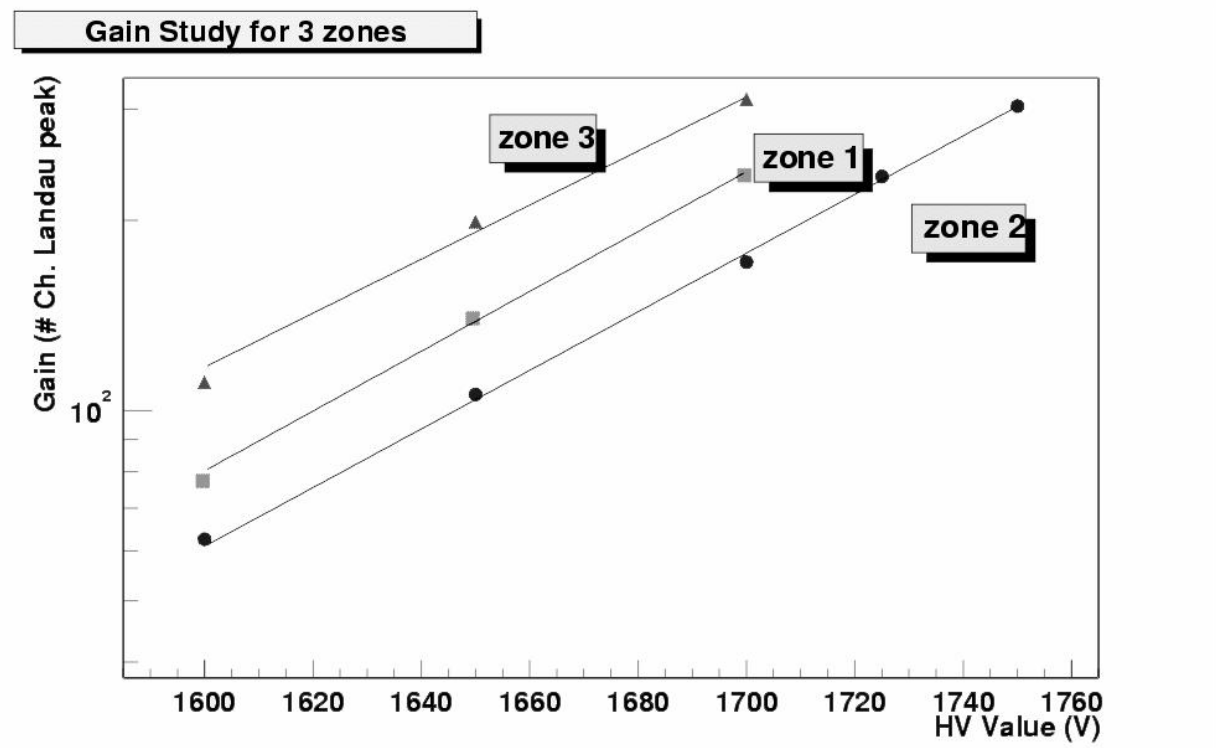


Figure 11: Gain values for different beam position versus high voltage values

The gain dispersion between zones 2 and 3 is about 1.8

Discussion on these different results:

Concerning the low value of the gain, several remarks can be done:

- the same gas factory with the same gas mixture has been used for our tests and for slat tests successively in the same beam period. No anomaly was observed for the slat gain. This insures that the gas mixture composition was correct at the entrance of the chamber.

- nevertheless due to the gas leakage, possible impurities, like H_2O , could affect the electron multiplication factor in the gas. Measurements performed at the exit of the bubbler revealed that O_2 contribution is lower than 1 ppm and H_2O about 700 ppm. These results are questionable because they have been done after several tens meters of Rilsan

For the gain homogeneity:

- local effects due to these impurities could be the source of the gain variation in different locations.

- the overpressure due to the gas circulation was fixed by the bubbler and was of the order of 0.5 mb. The theoretical calculation of the mechanical structure predicts a deformation around 80 μm in the centre of the chamber. Due to the leakage and to the high flux through the chamber, we could suspect an additional deformation. Measurements of this effect have been performed which was found negligible, as shown in figure 12.

- the gain value is directly related to the wire positions in the chamber and a default of positioning due to electrostatic forces could induce gain variation from wire to wire. Such an effect should be larger in the middle of the chamber where the wires are longer (up to 80 cm). An indication of these two previous effects can be seen in figure 13, where the gains are plotted for different measurements as a function of the distance to the centre of the chamber.

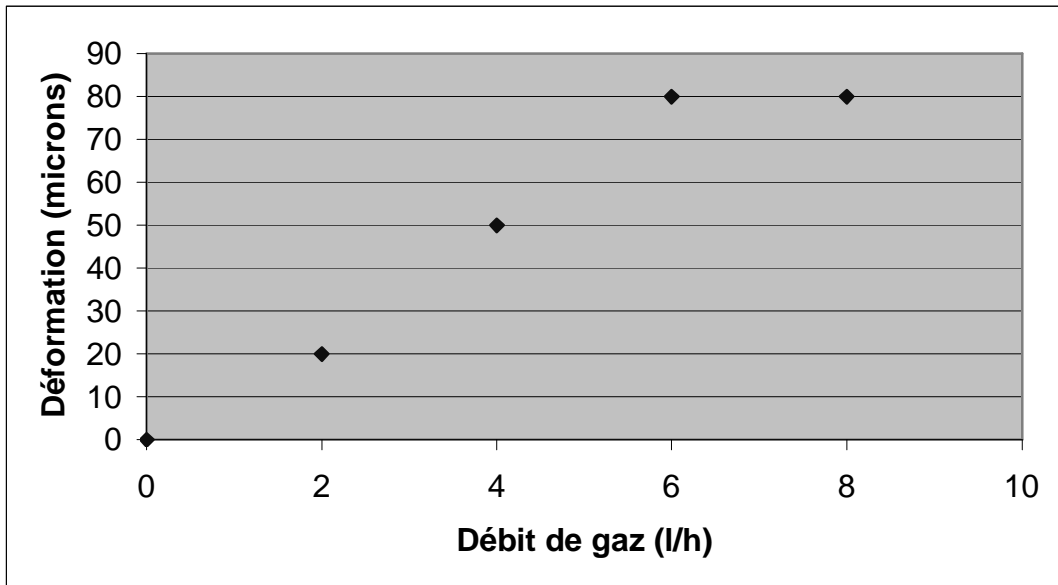


Figure 12: variation of the anode-cathode gap versus the gas flux in the centre of the chamber. The overpressure of 0.5 mb is obtained for a gas flux of 6 l/h.

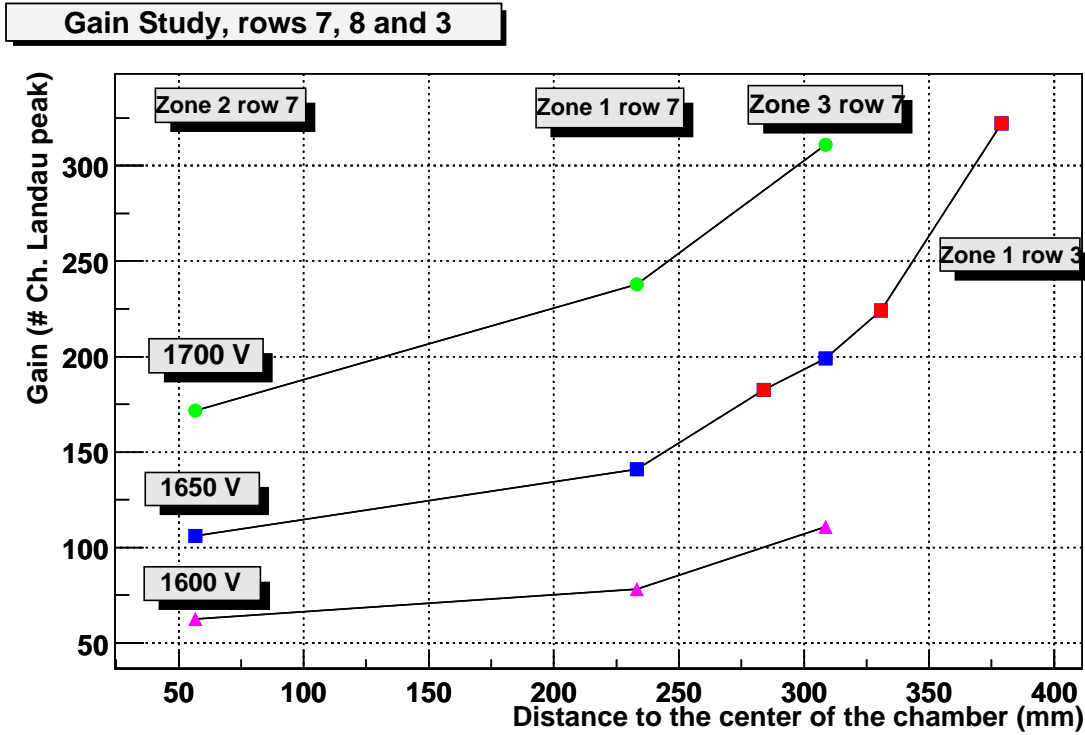


Figure 13: Gain as a function of the distance to the centre of the chamber for different high voltage values

6- Further analysis.

The 10 planes of the standard silicon trackers have been used to reconstruct the track in the two directions in a standard procedure previously described [1]. The accuracy of the construction is very good (of the order of 15 to 20 μm per plane). The extrapolation of the track on the quadrant0 cathode plane was calculated and used to study more carefully the charge distribution on the cathode pads. For the most central zone, the Y direction (along the wires) corresponds to the “bending” direction (i.e good resolution direction). So it is possible to study the spatial resolution. For the two others zones corresponding to “non-bending” architecture it is only possible to extract the position of the wires.

Results for the central zone.

- **Structure of the clusters.**

As usually done [1], the different configurations in the Y direction, for clusters of hit pads, are studied and the results for one measurement called “1” in figure 7, are reported in the table 2 as function of the high voltage. The analysis has been performed with the 3σ standard threshold on each individual pad charge.

High voltage (V)	1600	1650	1700
1 pad	1	0.41	0.35
2 adjacent pads	35.6	19	7.7
3 (or more) adjacent pads	63.3	80.3	91.3
1 saturated pad (central)	0.03	0.24	0.64

Table 2: Pad configuration repartition (percentage) versus high voltage values

Due to the dynamics range (reduced by a factor of about 3 compared to GASSIPLEX 1.5 μm used previously for the mock-up) the saturation effects are very small for all HV settings we have studied, and are found about 0.8 % at HV= 1700 V (see figure 14).

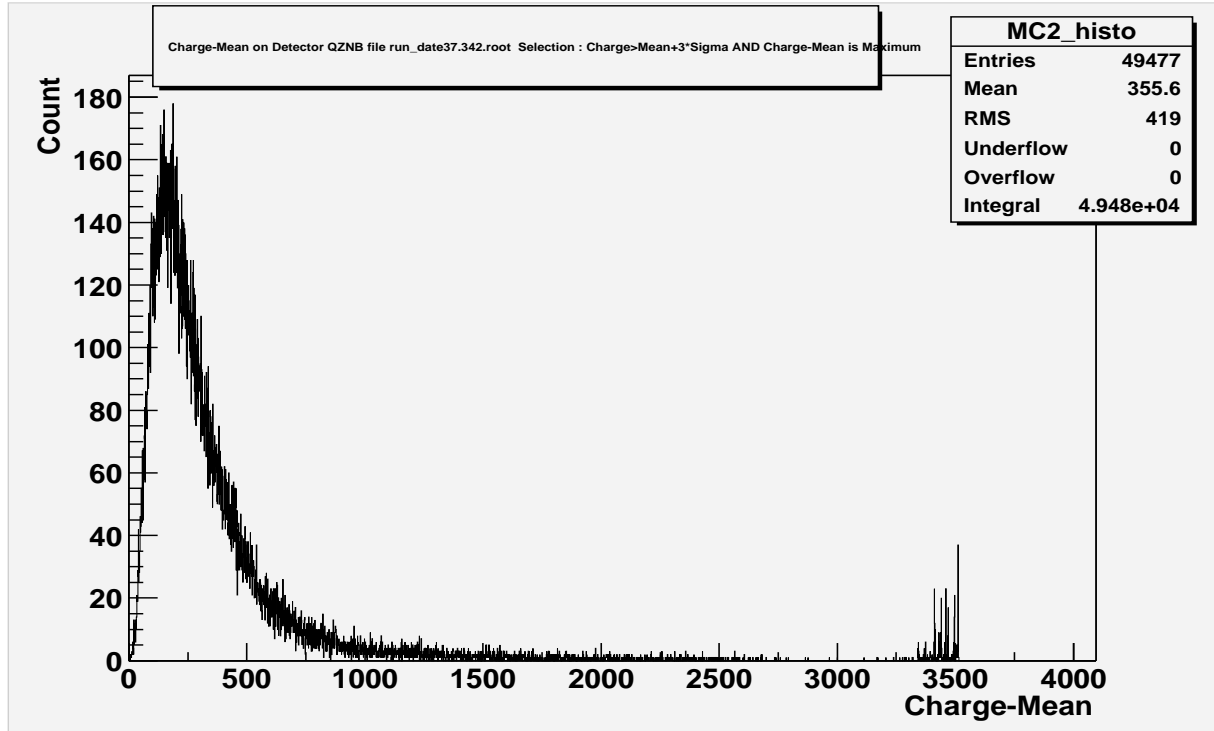


Figure 14: Histogram of the maximum charge of the clusters

Three adjacent pads or more (one central with the maximum charge and two lateral) is the predominant configuration. The configuration with two hit pads corresponds mainly to hits close to the edges of the pads in the y direction. In this case, the charge repartition on each pad has been calculated in the Mathieson model [1 and ref. therein] and found to be 1.27%, 48.7%, 48.7%, 1.27% in percentage of the total charge (the configuration is symmetric for a hit at the limit of two pads). This is a rough calculation ignoring the effect of the noise. Nevertheless, the 3σ mean cut corresponds roughly to 2.7 channels and will suppress all events for which the total charge is lower than approximately 212 ADC. For comparison the most probable value (MPV) of the measured total charge is 291 ADC at 1700 V (see fig 9) and 95 ADC at 1600 V. This explained the strong variation of the percentage of the two pads configurations versus the high voltage.

A complete simulation has been performed at 1600 V and 1700 V (see details for the procedure in ref. 1) using the following inputs:

- Hits generated randomly in the x and y direction with a uniform distribution.
- Landau charge distribution adjusted on the measured total charge.
- Noise level (1 ADC)
- 3σ threshold
- Mathieson induced charge distribution on the cathode plane with geometrical parameters used for the experimental analysis.

Results are summarized in table 3 and are very sensitive as discussed before to the Landau MPV position. A qualitative agreement with the experiment is observed.

High voltage	1600 V	1700 V
Percentage (%) for 2 pads configuration	44.0	5.4 - 6

Table 3 : Results of a simulation giving the percentage of two pads configurations in the y direction

The histogram of the number of hit pads per event is presented in fig. 15.

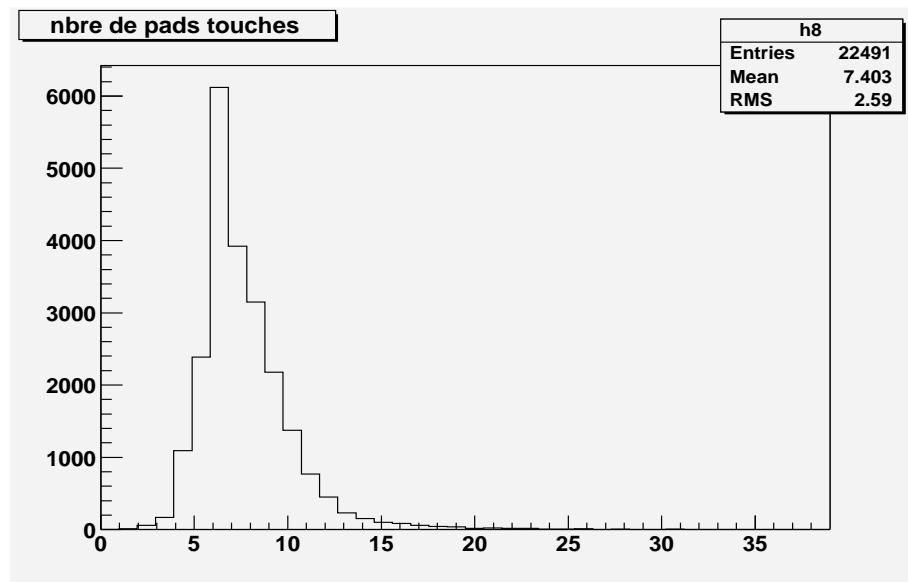


Fig 15: Histogram of hit pads/events. The standard 3σ cut has been applied.

The results are very comparable to the ones for the mock-up (taking into account a HV shift of 220 V previously discussed)

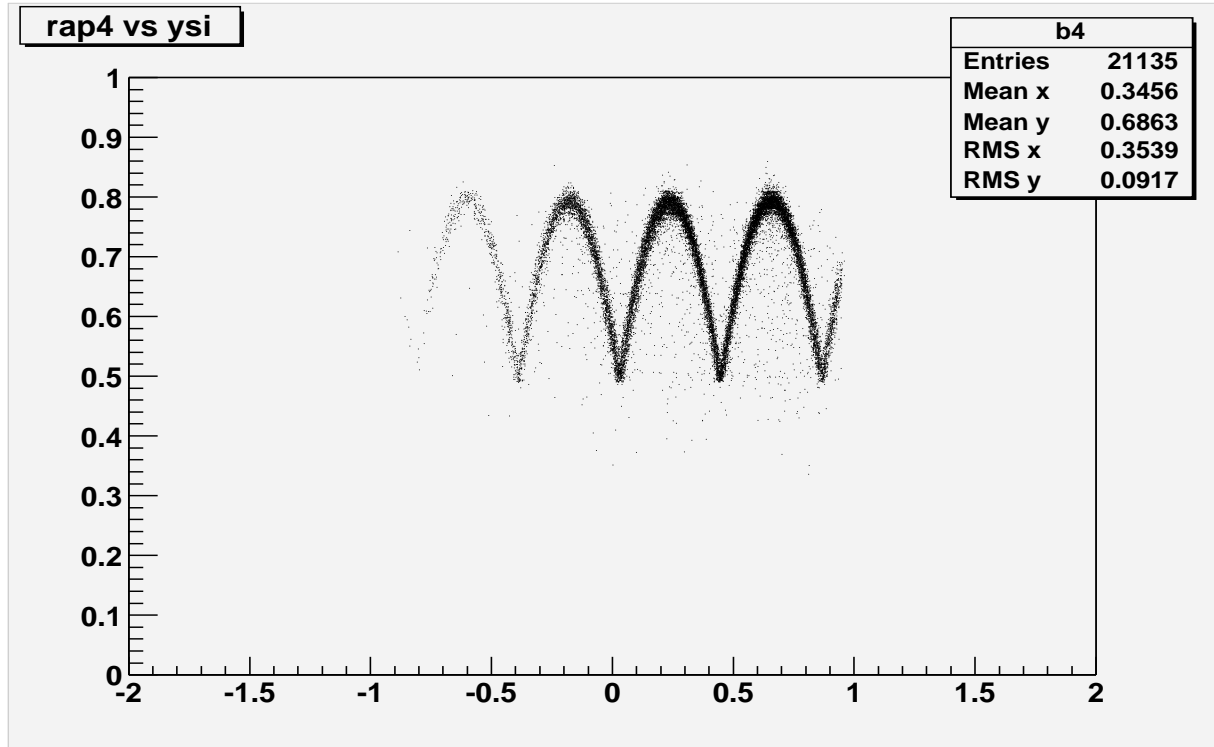


Fig 16: Ratio of the maximum charge divided by the sum of the three adjacent charges of the cluster

Using the silicon information of the position on the detector it is possible to plot (figure 16) the usual ratio of the maximum central charge divided by the sum of the three adjacent charges as function of the position. A fair agreement is observed with a rough simulation taking into account the geometrical parameters only.

- **Spatial resolution**

The spatial resolution has been extracted using the standard Mathieson fit [1] with the parameters $k_{3\text{ par}} = 0.49$ and $k_{3\text{ orth}} = 0.58$ which are the theoretical values for this geometry. The results are presented in table 4 and plotted in figure 18 as function of the high voltage values without the subtraction of multiple scattering contribution (estimated to $40\text{ }\mu\text{m}$).

High voltage (V)		1600	1650	1700
2 adjacent pads	Resolution (μm)	96.	84.6	82.7
	Efficiency (%)	34.2	18.4	7.4
3 adj. pads or more	Resolution (μm)	89.6	84.8	83.1
	Efficiency (%)	58.2	75.0	86.2
Global	Resolution (μm)	92.	85.	83.4
	Efficiency (%)	92.4	93.5	93.7

Table 4 : Spatial resolution and efficiencies (calculated in a $\pm 300 \mu\text{m}$ window around the position given by the silicon tracker)

The overall achieved resolution is about $80 \mu\text{m}$ (see figure 17).

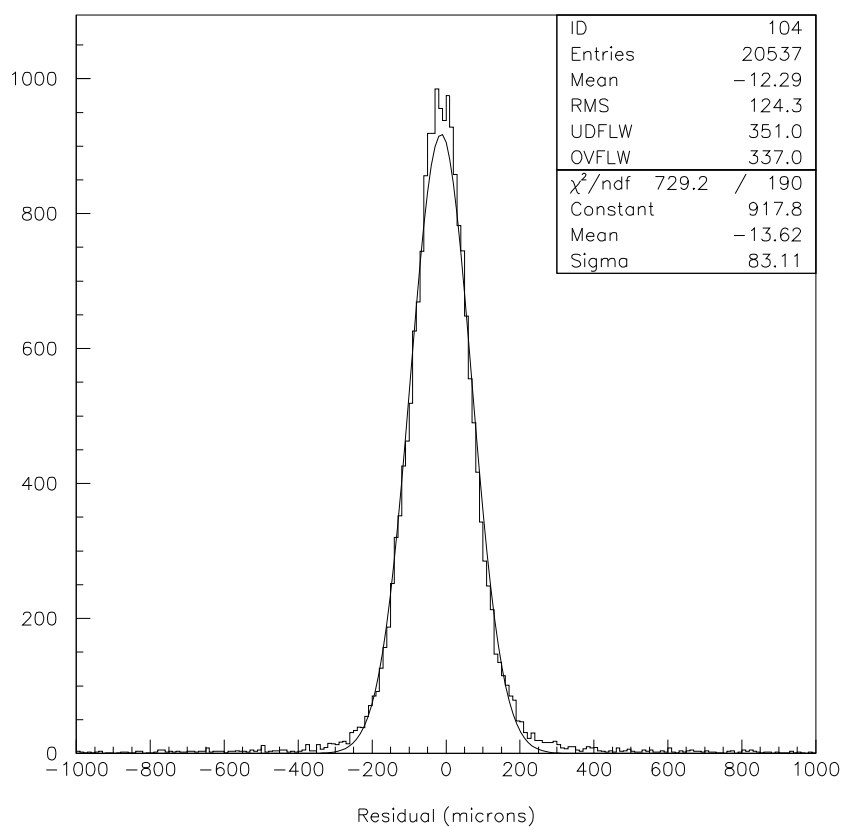


Figure 17: Spatial resolution (cm) for 3 pads configurations obtained for HV = 1700 V without multiple scattering subtraction

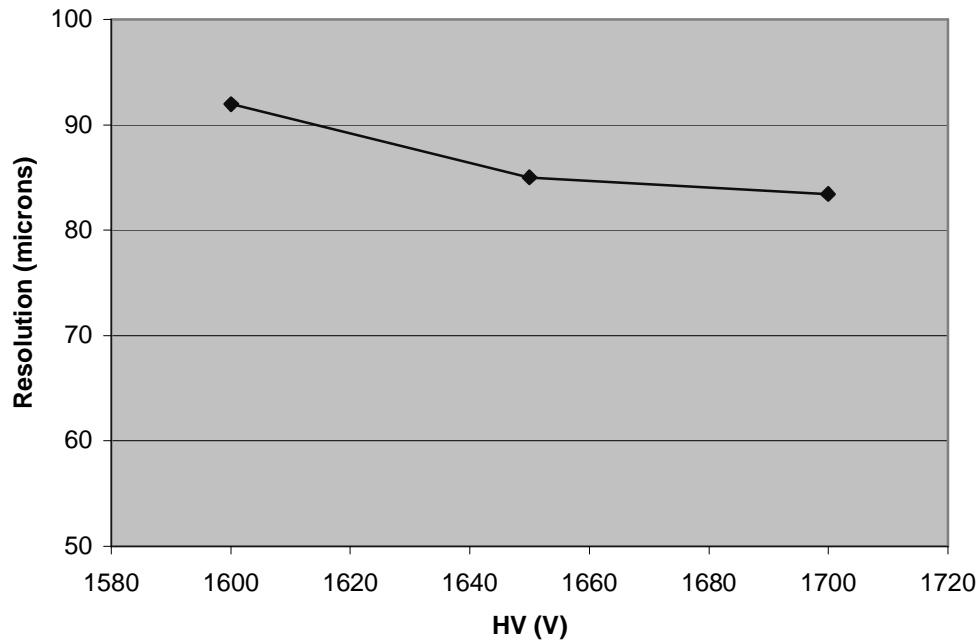


Figure 18: Spatial mean resolution (without multiple scattering subtraction) as function of high voltage values.

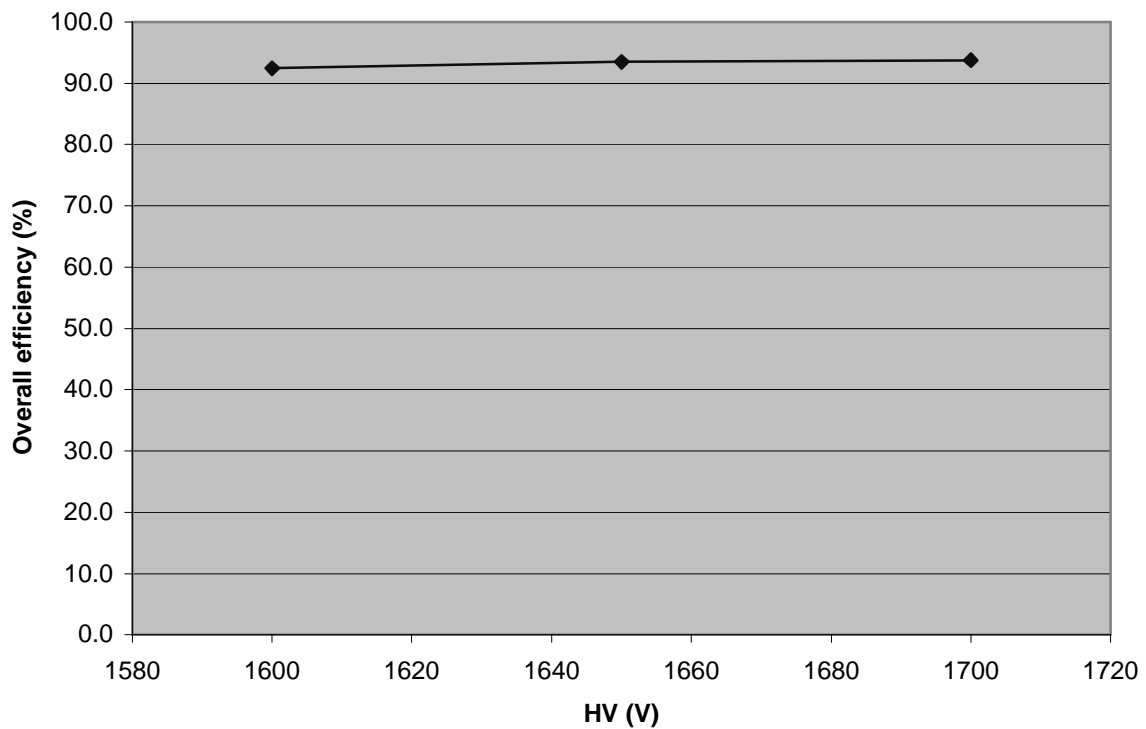


Figure 19: Overall efficiency as function of the high voltage values.

It can be noticed that an efficiency plateau is reached around 1650-1700V. Unfortunately, no measurements have been performed at lower high voltage values. The detector operation becomes instable at higher values.

Conclusion: Most of the results which are presented before are extracted for the central zone. The in-beam tests have been globally successful and have validated the choice of the geometrical parameters. Nevertheless a better quality control has to be insured during the

mounting phase and a spacer will be fixed in the centre of the quadrant in order to maintain mechanically the gap between the cathode planes to the nominal value. Despite the lack of gain in the centre of the chamber, the physical performances (efficiency and resolution) fulfil the requirements. Mechanical improvements will insure a safer operating mode.

We are indebted to INTAS (contract N⁰ 538) for its financial support during this work

[1]- Summary of the R&D performed at IPN Orsay for the ALICE dimuon tracking chambers, N. Willis et al. Internal report IPNO DR

[2]- Rob Veenhof, private communication